

RECEIVED BY OSTI

JUN 07 1985

LA-UR--85-1587

DE85 012679

CONF-850504--128

Los Alamos National Laboratory is operated by the University of California for the United States Department of Energy under contract W-7405-ENG-36

TITLE THE RF POWER SYSTEM FOR THE CHOPPER/BUNCHER SYSTEM ON THE  
NBS-LOS ALAMOS RTM

AUTHOR(S): L(loyd) M. Young and D(avid) R. Keffeler

SUBMITTED TO 1985 PARTICLE ACCELERATOR CONFERENCE  
Accelerator Engineering and Technology  
Vancouver, British Columbia  
May 13-16, 1985

#### DISCLAIMER

This report was prepared as an account of work sponsored by an agency of the United States Government. Neither the United States Government nor any agency thereof, nor any of their employees, makes any warranty, express or implied, or assumes any legal liability or responsibility for the accuracy, completeness, or usefulness of any information, apparatus, product, or process disclosed, or represents that its use would not infringe privately owned rights. Reference herein to any specific commercial product, process, or service by trade name, trademark, manufacturer, or otherwise does not necessarily constitute or imply its endorsement, recommendation, or favoring by the United States Government or any agency thereof. The views and opinions of authors expressed herein do not necessarily state or reflect those of the United States Government or any agency thereof.

By acceptance of this article the publisher recognizes that the U.S. Government retains a nonexclusive, royalty-free license to publish or reproduce the published form of this contribution or to allow others to do so for U.S. Government purposes.

The Los Alamos National Laboratory requests that the publisher identify this article as work performed under the auspices of the U.S. Department of Energy.

**Los Alamos** Los Alamos National Laboratory  
Los Alamos, New Mexico 87545

THE RF POWER SYSTEM FOR THE CHOPPER/BUNCHER SYSTEM ON THE NBS-LOS ALAMOS RTM\*

L. M. Young and D. R. Keffeler, AT-1, MS H817  
Los Alamos National Laboratory, Los Alamos, NM 87545 USA

## Summary

The rf power system and its closed-loop feedback control for the racetrack microtron (RTM) chopper/buncher system are described. Measurements made on the response of the feedback system to external perturbations will also be reported.

## Introduction

The 100-keV injector for the National Bureau of Standards (NBS)-Los Alamos racetrack microtron (RTM)<sup>1</sup> uses two square deflection cavities and a buncher cavity. The deflection cavities operate in the TE<sub>102</sub> and TE<sub>201</sub> modes,<sup>2</sup> and the buncher operates in the TM<sub>010</sub> mode. Figure 1 illustrates how the beam is deflected off axis into a spiral by the deflection cavity; the beam traces a circle on the chopping aperture. A 60° circumferential slit in the chopping aperture allows only 1/6 of the input beam to pass through. A pair of thin-gap lenses centered on this aperture focuses the chopped beam back to the axis at the second deflection cavity. The second half of the chopper section is a mirror image (centered on the aperture) of the first half. If rf phase and amplitude are adjusted properly, the transverse momentum imparted to the beam by that of the first deflection cavity will be exactly cancelled by that of the second deflection cavity so that the beam becomes coaxial after the second deflection cavity.

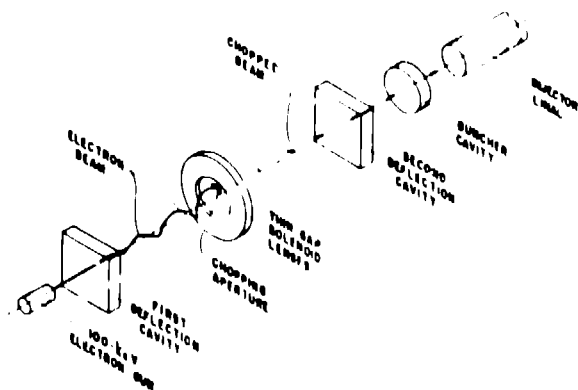


Fig. 1. The chopper/buncher system for the JLS Los Alamos RIM. An electron beam from a 100-keV electron gun is deflected by a rotating magnetic field in the first deflection cavity, forming a spiral that traces a circle on the chopping aperture. The thin-gap lenses focus the spiraling beam back to the axis at the second deflection cavity. There, it is deflected along the axis by a rotating magnetic field that is adjusted to exactly cancel the transverse kick it was given by the first deflector.

The 2380-MHz bunching cavity decelerates the head of the 60° long bunch from the chopping system and accelerates the tail. This action reduces the length of the bunch to about 10° at the entrance to the injector linac. The square deflection cavity deflects the beam into circles on the chopping aperture by simultaneous excitation of the 1E<sub>102</sub> and 1E<sub>201</sub> modes. One mode deflects the beam horizontally and the other vertically. When the modes are excited to equal amplitude with relative rf phase difference of 90°, the beam scribes a circle on the chopping aperture. This chopping system causes very little emittance growth of the

\*Work supported by the US Department of Energy.

electron beam, but only if the phases and amplitudes of the rf power in each deflection cavity is controlled very accurately. Therefore, each deflection cavity uses two rf power sources, each with its own phase and amplitude control. The chopper/buncher system uses a total of five rf power sources with five separate amplitude and phase feedback-control loops. These amplitude and phase feedback loops are all identical.

## Phase and Amplitude Feedback Controls

The rf system is shown in Fig. 2. The rf source is derived from a voltage-controlled crystal oscillator (VCCO) at 148.75 MHz, which is then frequency multiplied by 16 to 2380 MHz. The frequency of this VCCO can be adjusted  $\pm 0.1\%$  with a  $\pm 5$ -V control signal. The rf source has phase noise from the multiplication; therefore, an oscillator is phase locked to this source. The output of this phase-lock oscillator has very little phase noise.

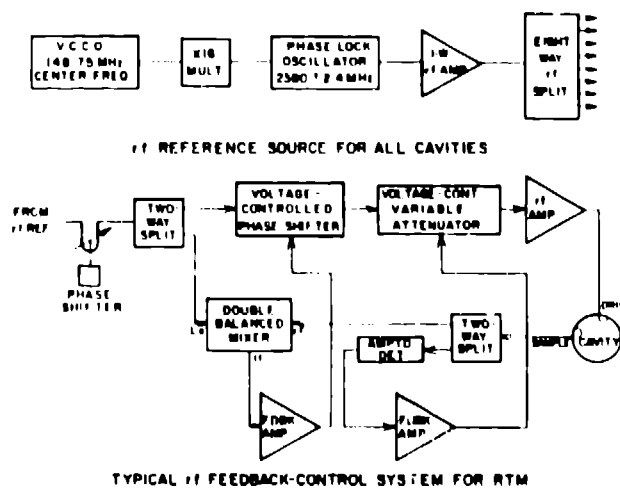


Fig. 2. A common rf reference source is used for all the cavities in the RIM. Each of the eight outputs of the rf reference source is used as an input to a feedback control system. Each cavity has its own feedback system.

A good rf source without phase noise is required for the RIM because there are many cavities in the RIM and all must operate at constant phase with respect to each other. A noisy rf reference source would prevent accurate phase control and measurements. An eight-way splitter on the rf source provides the rf reference for all the rf control loops in the RIM. These rf reference signals go through stepping-motor driven line stretchers to provide phase adjustment for each device. In each controller, the rf reference is split with one output going to a double-balanced mixer (DBM) and the other going through a voltage-controlled phase shifter and a voltage controlled attenuator to one or more amplifiers required to drive a particular cavity. The voltage controlled phase shifter has a phase range of  $-270^\circ$  for a control voltage swing from 0 to 30 V. The voltage controlled attenuator has a range of  $\sim 60$  dB, with an attenuation change of  $\sim 10$  dB/V from 0 to 6 V. These devices are not perfect in that the phase shifter has a small change of attenuation versus control voltage, and the attenuator has a small amount of phase shift versus control voltage. The small interaction between amplitude and phase control has not caused any problems with operation and control of the chopper buncher.

A pickup loop in the cavity samples the rf cavity fields close to the outer wall. This rf signal is split with one output going to an amplitude detector (low-barrier Schottky diode detector). The output of this detector is proportional to the rf amplitude in the cavity. The other output goes to the DBM, where it is mixed with the rf reference. The output of the DBM will consist of two frequencies: the sum and the difference. The sum frequency can easily be removed with a low-pass filter. Because the two inputs to the DBM are the same frequency, the frequency of the difference is zero, which is a dc signal. This dc signal provides the phase information and can be represented by  $A \times \sin(\Delta\phi - \phi_c)$ , where  $A$  is a function of the rf power of the two signals,  $\Delta\phi$  is the phase difference of the two signals, and  $\phi_c$  is a constant. By choosing to operate the phase-control loop with the output of the DBM zeroed,  $\Delta\phi$  must be equal to  $\phi_c + n \times 180^\circ$ , where  $n$  is an integer and  $A \neq 0$ . The voltage signals from the amplitude detector and the phase detector (the DBM) are amplified by the feedback amplifiers. The amplified signals are then used to drive the phase shifter and the variable attenuator.

The operational amplifier (OP-AMP) chosen for the feedback amplifiers is the LF356N. It has a gain bandwidth of 4 MHz and a low-input offset voltage temperature coefficient of  $\leq 3 \mu\text{V}/^\circ\text{C}$ , which results in a low-input offset drift that is important for good stability of the amplitude and phase. Figure 3 shows a simplified schematic of the feedback amplifiers. All the OP-AMPs are in an inverting configuration. The phase feedback amplifier requires only two OP-AMPs. The first is the integrating stage, and the second provides a voltage output between 0 and 23 V. The 0- to 23-V range utilizes most of the  $270^\circ$  of phase shift available from the phase shifters because the phase shifters are near saturation for control voltages between 23 and 30 V.

Because the output of the DBM is bipolar (with two zero-crossing points) versus phase difference between the rf reference and the rf sample, one of the crossing points will result in positive and the other in negative feedback. The circuit automatically will

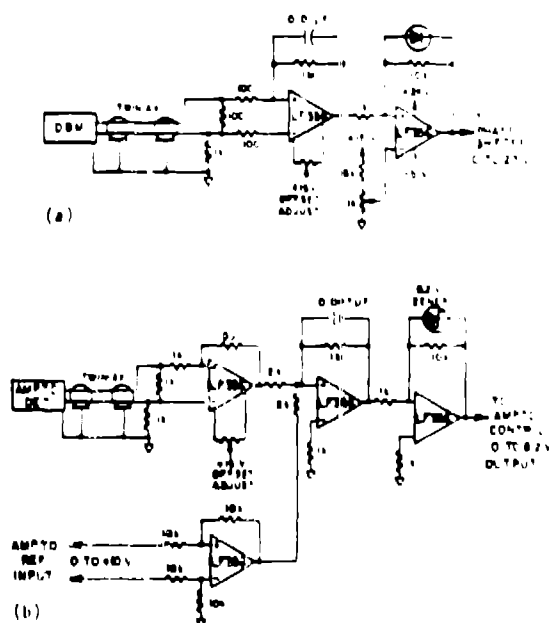


Fig. 3. The feedback amplifiers for (a) the phase control and (b) the amplitude control use the same methods to reduce noise pickup on the input. The DBM and the amplitude detector are only grounded by the shield of the twin ax of the analog ground of the feedback amplifiers. The DBM and the amplitude detectors are isolated from the ground of the rf system by dc blocks (not shown).

select the appropriate zero-crossing point that results in negative feedback for the phase control. The zero crossing that results in positive feedback is unstable, and the circuit will try to change the phase to the nearest zero crossing with negative feedback. It is possible to set up the phase-control loop with the two zero-crossing points of the DBM within the  $270^\circ$  range of the phase shifters. Then, it is possible for the phase-control loop to latch on the wrong side of the zero-crossing point with positive feedback. To eliminate this possibility, a stepping-motor controlled phase shifter is included in the phase-control loop to adjust the phase-control range to encompass only the negative-feedback, zero-crossing point.

The output of the amplitude detector is unipolar; therefore, the polarity of the feedback is fixed. The amplitude detector has a negative output, and the variable attenuator increases the attenuation for a positive control voltage, which requires the feedback amplifier to be inverting. In this system, the best way to achieve the inversion is with three inverting OP-AMPs, consisting of an input buffer, an integrator, and an output buffer.

An example of a simple feedback-control system is shown schematically in Fig. 4(a). Figure 4(b) shows this system open loop and Fig. 4(c) shows the Bode approximation of the open-loop gain-magnitude frequency response. Figure 4(d) shows the corresponding Bode approximation of the phase shift. The open-loop gain must be less than 1 when the phase shift exceeds  $180^\circ$  or the feedback loop [Fig. 4(a)] will oscillate. In this example,  $A$  is an operational amplifier with one pole at frequency  $f_p$ . This pole introduces a phase shift that equals  $90^\circ$  for all frequencies greater than  $\sim 10 f_p$ . The load will introduce additional phase shift that causes the total phase shift to exceed  $180^\circ$  at a high frequency.

The loop gain of the system must be less than 1 when this additional phase shift causes the total phase shift to exceed  $180^\circ$ . The phase margin is defined as the amount the phase shift is less than  $180^\circ$  at the frequency when the loop gain equals 1.

The feedback amplifiers are configured as integrators only. Because the gain response must fall off uniformly at 20 dB/decade (resulting in a  $90^\circ$  phase margin in the feedback amplifier) and must have a unity-gain crossover that provides a satisfactory phase margin, the integrator capacitance is chosen to

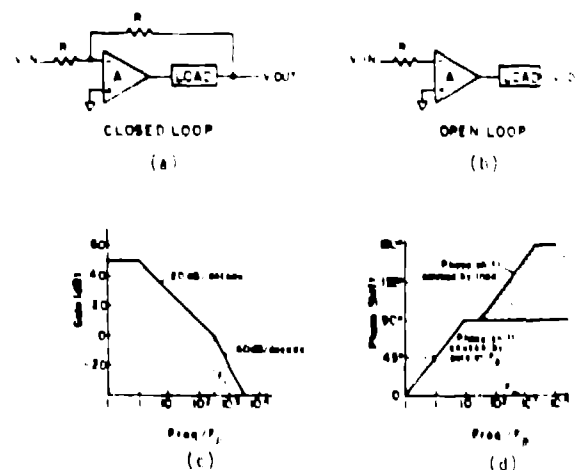


Fig. 4. The basic components of a feedback system are shown in the normal closed loop configuration, (a). If the feedback loop is open (b), the Bode approximation of the gain versus frequency is shown in (c), and the phase shift of the system is shown in (d). The amplifier  $A$  has a pole at frequency  $f_p$  and the load has a pole at frequency  $f_l$ . A feedback system is stable if the total phase shift in the feedback loop is less than  $180^\circ$  for frequencies at which the gain is greater than unity. If this condition is violated, the system will oscillate.

give a unity-gain crossover at the desired frequency. The feedback amplifiers are very easy to adjust because only one variable needs adjusting and that one is the frequency at which the loop gain is unity. The optimum size of the integrator capacitor depends on the gain of the loop external to the feedback amplifier. Because the variable attenuator is linearized, the feedback gain in the amplitude control loop is proportional to the magnitudes of the amplitude detector signal. The feedback gain in the phase-control loop also depends on the amplitude of the rf and the magnitude of the phase-control voltage. The phase shifter is not linearized and has more gain for phase-control voltages near 0 V than for control voltages near 30 V. The integrator capacitor used in the feedback amplifier gives a unity-gain crossover at ~40 kHz (see Fig. 5) for both control loops when there is a 0.4-V signal from the amplitude detector, which corresponds to an amplitude reference voltage of 2 V.

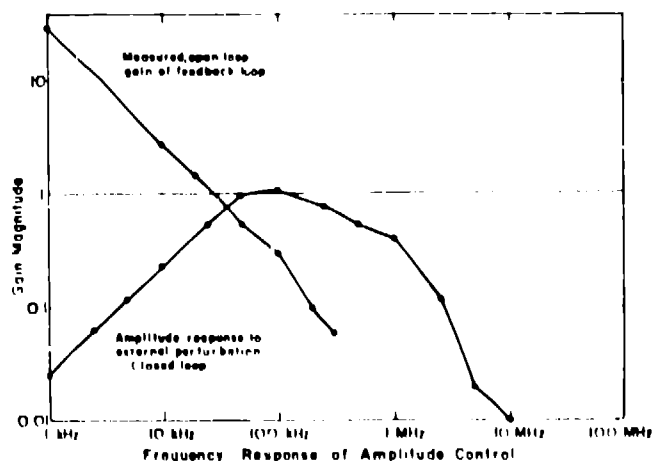


Fig. 5. Measurements of gain versus frequency with the amplitude feedback system operating open loop are indicated. With the feedback system operating in a closed loop configuration, a perturbation was applied to the load. The resulting ratio of the change in the rf amplitude to the amplitude of the perturbation versus frequency is shown.

Figure 5 shows the open loop gain of the amplitude feedback loop, which was measured with an ~0.3 V signal level from the amplitude detector. Note that the unity gain crossover occurs at ~30 kHz. For a 0.4 V signal, the unity gain crossover occurs at ~40 kHz, and so on. The amplitude response was measured with the loop closed and with a 0.4 V signal from the amplitude detector. This measurement was made by inserting an external, voltage controlled attenuator in the rf feedback loop and comparing the response of the rf amplitude signal with the feedback loop in control to the response without the feedback loop in control. If the application required better control for perturbations near 100 kHz, higher speed OP-AMPs would have to be used in the feedback amplifiers; however, for the RIM this should not cause any difficulty because there should not be any source of perturbation at this frequency. Good control is obtained at all other frequencies. The open loop gain of only the feedback amplifier was measured and compared to the open loop gain calculated with the Bode approximation. The gain drops off slightly faster than the Bode approximation predicts from the OP-AMP specifications. This measurement of the open-loop gain indicates that in this circuit, the OP-AMPs have a unity gain bandwidth of ~3 MHz.

The measured open loop gain of the phase control loop essentially is identical to the gain of the amplitude feedback loop shown in Fig. 5. This measurement was made with a 0.3 V signal on the amplitude detector and with the phase control voltage near the middle of

the control range. The gain is higher for the control voltage near zero and lower for the control voltage near 23 V. The phase response was measured by inserting a voltage-controlled phase shifter in the rf feedback loop and modulating the voltage on this external phase shifter. The response measurement was then made by comparing the phase perturbation with and without the phase feedback control working. The phase response is also essentially identical to the amplitude response shown in Fig. 5. This measurement shows that at 100 kHz, the feedback control has little effect on the perturbation, but that good control is obtained at all other frequencies. The response drops off above 100 kHz for both amplitude and phase because the high-Q cavity attenuates the perturbation.

Figures 6 and 7 show the amplitude and phase response to a square-wave perturbation. The perturbations are shown on the top trace, and the resulting effect on the amplitude and phase are shown on the bottom traces of Figs. 6 and 7, respectively. The scale on the perturbation and the response are the same. The perturbation causes an unwanted change in the amplitude and phase, but the amplitude and phase excursion is only about half that of the perturbation, and the amplitude and phase are returned to their desired value within ~10  $\mu$ s by the feedback controls.

Preliminary tests show that this rf system controlled the amplitude to within 0.1% and the phase to within 1°. Short-term variations in the amplitude and phase were <0.04% in amplitude and <0.1° in phase in a test system.

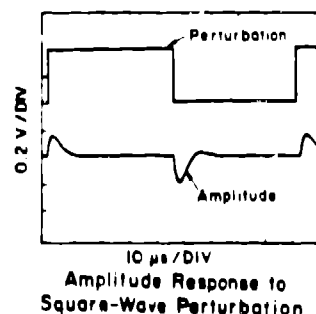


Fig. 6. An oscilloscope trace of a square-wave perturbation and the resulting effects on the amplitude of the rf in a cavity. The size of the square-wave perturbation shown is adjusted to equal the resulting perturbation of the amplitude signal with the feedback turned off.

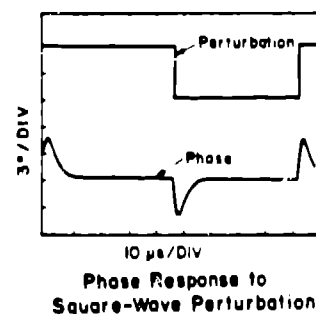


Fig. 7. An oscilloscope trace of a square-wave perturbation and the resulting effects on the phase of the rf in a cavity. The size of the square-wave perturbation shown is adjusted to equal the resulting change in phase with the feedback turned off.

## Conclusion

This rf system was installed on the RIM at NBS in March 1984 and has operated satisfactorily during tests with beam in the chopper/buncher system. The electron beam was observed to scribe a circle on a view screen at the chopping aperture. The thin-gap lenses focused the beam back to the axis at the second deflection cavity. The rf fields in the second deflection cavity were adjusted to exactly cancel the transverse deflection it was given by the first deflection cavity. This cancellation of the transverse deflection was observed by a view screen beyond the second deflection cavity.

## References

1. S. Penner, R. L. Ayres, R. L. Cutler, P. H. Debenham, L. H. Lindstrom, D. L. Mohr, J. I. Rose, M. P. Unterwiesing, M. A. D. Wilson, R. Diddle, L. R. Martin, J. L. Stovall, P. J. Tellerico, L. Wilkerson, and L. M. Young, "Progress Report on the NBS/Los Alamos RIM," these proceedings.
2. Jacob Maimson, "Optimization Criteria for Standing Wave Transverse Magnetic Deflection Cavities," Proc. 1966 Linear Accelerator Conf., October 3-7, 1966, Los Alamos Scientific Laboratory report LA 3509 (December 1966), 303.